Growth phase influences virulence in *Candida auris* systemic infection models

Michael J. McFadden, Juliet A.E. Anku, Faith A. Davis, Teresa R. O'Meara[†]

Affiliations:

Department of Microbiology and Immunology, University of Michigan, Ann Arbor, MI 48109, USA.

[†] Corresponding author: Correspondence to Teresa R. O'Meara (tromeara@umich.edu)

Abstract

Candida auris is a growing public health concern, capable of causing long-term contamination of healthcare settings, skin colonization, and life-threatening bloodstream infections. However, *C. auris* pathogenesis is not well understood, which is exacerbated by limitations and discrepancies in existing animal infection models. Further, the effects of *C. auris* growth phase on virulence have not been examined, despite growth phase being linked to virulence in many bacterial species. To address this question, and to develop an immunocompetent murine model of infection, we directly compared log and stationary phase *C. auris* systemic infection in immunocompetent C57BL/6J mice at high and low doses of infection. Systemic infection with high dose log-phase *C. auris* results in rapid mortality between 2 hours and 1 day post infection, whereas stationary phase *C. auris* results in significantly extended survival. However, at low doses of infection, there was no difference in mortality kinetics between log and stationary phase cells. We observed that *C. auris* initially colonizes multiple organs but is rapidly cleared from the lungs and spleen, while kidney fungal burdens remain stable. Decreased fibrinogen levels and blood clotting in the lungs of mice infected with high dose log-phase *C. auris* suggest that blood clotting may drive rapid mortality, potentially associated with increased β-glucan exposure and mannan abundance observed in log phase *C. auris*. These results will inform the development of a more standardized animal model of systemic *C. auris* infection, which can be used to reveal key aspects of *C. auris* pathogenesis.

Importance

Despite its growing medical importance, there is limited understanding of *Candida auris* pathogenesis, due in part to limitations of existing laboratory models of infection. To develop a more complete understanding of factors that contribute to *C. auris* pathogenesis, it will be

necessary to establish consistent parameters for animal models of infection. To address this need, we directly compared log and stationary growth phases on *C. auris* pathogenesis in immunocompetent C57BL/6J mice using a single Clade I isolate. At a high dose of infection, host survival was dramatically different between log or stationary phase *C. auris*, suggesting that growth phase can affect *C. auris* virulence. These differences correlated with increased exposure of pathogen-associated molecular patterns in the *C. auris* cell wall in log phase cells. These results will be instrumental in the future development of standardized animal models to study *C. auris* pathogenesis.

Introduction

Candida auris is an often multidrug resistant invasive species within healthcare settings that also can cause systemic infection with mortality rates higher than 30% (1, 2). *C. auris* pathogenesis is not well understood due to its recent emergence and the existence of comorbidities in many infected patients, as well as an incomplete understanding of host-pathogen interactions and pathology within sites of *C. auris* infection (3–5). While animal models have been of great utility in understanding the relative contribution of specific fungal mutants to virulence (6–9), there is not a standard animal model for *C. auris* disseminated disease. The immunocompromised model of *C. auris* was initially developed as a physiologically relevant model of systemic infection, with a particular focus on its utility for testing of antifungal compounds (10) or specific types of immunocompromise (11). Immunocompetent models of *C. auris* infection have also been developed in ICR outbred mice (12), BALB/c (13), and C57BL/6J (3, 4) backgrounds, with varying kinetics and rates of mortality. Additionally, *C. auris*-specific factors, such as strain background are likely a major source of variability between publications as evidenced by our recent work showing significant differences in virulence between two closely related clade I isolates (6). Beyond strain differences, work in bacterial pathogenesis has demonstrated that

growth phase can also influence virulence, but the effects are species specific and were determined empirically. For example, for *Legionella* and *Brucella*, entry into stationary phase is associated with increases in virulence factor expression (14, 15), but for *Salmonella* and *Streptococci*, it is the exponential growth phase that is associated with virulence (16, 17). Therefore, we sought to determine the effects of *C. auris* growth phase and dosage on host survival and pathology using a single strain of *C. auris* and a single genetically tractable and immunocompetent murine model of systemic infection.

At a high dose of systemic *C. auris* infection, we observed that log/exponential phase fungi cause rapid mortality compared to stationary phase fungi, which cause mortality over the course of several days. These differences in mortality may stem from rapid extensive blood clotting caused by log phase *C. auris*, as we observed decreased serum fibrinogen levels and blood clotting in the lungs. Exponentially growing *C. auris* cells had increased β-glucan exposure and mannan abundance, potentially promoting detection by host cells and triggering blood clotting and rapid mortality. However, differences in mortality observed at a high dose of infection were ablated at a low dose of infection, in which mice survived over the course of multiple weeks. We recovered *C. auris* from the lungs, spleen, and kidneys early after infection, but over time, only the kidneys maintained a substantial fungal burden. Together, these results suggest that growth phase can have dramatic effects on survival during systemic *C. auris* infection. Additionally, our work provides new insight into *C. auris* disease progression and will be helpful in establishing more standardized approaches to modeling *C. auris* infection in immunocompetent mouse models.

Results and Discussion

Comparing the Effect of Candida auris Growth Phase on Survival Kinetics and Fungal Burden in Organs

To assess whether growth phase affects virulence during systemic *Candida auris* infection, we compared infection outcomes in an immunocompetent murine model using log or stationary phase *C. auris* cultures at a high and low dose of infection ($5x10^7$ and $1x10^6$, respectively) using the AR0382 (B11109 clade 1) isolate (Fig. 1A). Following intravenous infection, each group was monitored for several hours for the onset of disease symptoms. Interestingly, a majority of the cohort infected with a high dose of log phase *C. auris* rapidly declined in health, becoming moribund and showing labored breathing within 2 hours of infection, resulting in humane sacrifice. None of the mice in this group survived beyond the first day post-infection (Fig. 1B). In contrast, mice infected with a high dose of stationary phase *C. auris* survived significantly longer than their log phase-infected counterparts, with onset of mortality starting at day 2 post-infection and full cohort mortality at day 6 post-infection (Fig. 1B). However, at the low dose of infection, we did not observe any significance in mortality between the log and stationary phase infection cohorts (Fig. 1C). These data suggest that the growth phase of *C. auris* affects pathogenesis in murine infection models specifically at a high dose of infection.

We measured the fungal burden in the lungs, kidneys, and spleen post-mortality in each cohort. In the high dose log-phase *C. auris*-infected cohort, which had very rapid mortality, we observed a significantly higher fungal burden in the lungs than in the stationary phase cohort, while there was no difference in burden in the kidneys or spleen (Fig 1E, F). However, the difference observed in lung fungal burden is likely a product of survival kinetics, rather than colonization, as the fungal burden in the lungs appeared to sharply decrease over time (Fig. 1G). In low dose cohorts, which survived significantly longer than high dose cohorts, we recovered very few fungal colonies from the lungs, indicating that *C. auris* is effectively cleared from the lungs over time (Fig. 1J).

Similarly, fungal burden in the spleen showed a decreasing trend at day 7 in the high dose cohort (Fig. 1H) and was generally low at the time of mortality in the low dose cohorts (Fig. 1K), consistent with clearance from these organs over time. In contrast, fungal burden in the kidneys remained consistent over time in both the high dose (Fig. 1I) and low dose cohorts (Fig. 1L). Together, these data suggest that *C. auris* disseminates to multiple organs after systemic infection but is cleared from the lungs and spleen, while fungal burden remains steady over time in the kidneys.

High Dose Systemic Infection with Log Phase C. auris Causes Rapid Blood Clotting.

We next sought to further understand the differences in mortality observed between log and stationary phase *C. auris* during systemic infection at a high dose. We noted animals that rapidly succumbed within the log phase high dose cohort exhibited blood clotting while performing cardiac puncture, a common feature of sepsis (18). Indeed, ELISA data showed decreased Fibrinogen levels in the plasma of this cohort (Fig. 2A), consistent with Fibrinogen being converted to insoluble Fibrin to form clots (19). Interestingly, levels of proinflammatory cytokines TNF, IL-6, and IL-1β were similar between the log and stationary phase high dose cohorts (Fig. 2B-D), suggesting blood clotting, rather than a cytokine storm, drives rapid mortality after systemic infection with log phase *C. auris*. Blood clots could also be observed in hematoxylin and eosin (H&E)-stained lungs from the log-phase infected cohort (Fig. 2E). Together, these data suggest that rapid blood clotting causes mortality after systemic infection with log phase *C. auris* at high dose.

We hypothesized that *C. auris* growth phase may affect the composition of the cell wall, triggering differential recognition and leading to septic shock. Therefore, we measured the major cell wall components chitin, mannan, and exposed β-glucan in log or stationary phase *C. auris*. Flow cytometry analysis revealed that log phase *C. auris* showed higher β-glucan exposure than stationary phase (Fig. 2F, I) and two distinct populations of high and low mannan cells, compared

to stationary phase, which showed a single peak with intermediate intensity (Fig. 2G, J). Mannan binding lectin-associated serine proteases can trigger blood clotting (20), revealing one possible mechanism by which the high mannan log phase *C. auris* may trigger rapid mortality at a high dose. In contrast, chitin levels were similar between log phase and stationary phase *C. auris* (Fig. 2H, K). These results reveal changes to the composition of the cell wall and exposure of pathogen associated molecular patterns in log phase *C. auris* cells, which may drive the immunopathological response and mortality observed during systemic infection at a high dose. Together this work establishes virulence differences between stationary and log phase *C. auris* at high doses and indicates that the development of a standardized murine infection system, including controlling for fungal growth phase, will be important for future studies examining *C. auris* pathogenesis.

Methods

***Candida auris* growth conditions.** *C. auris* strain CDC-AR0382 (B11109) was grown in YPD liquid media (1% yeast extract, 2% peptone, 2% dextrose) with constant agitation. After 16 hours, stationary phase cultures were sub-cultured by diluting to OD600 of 0.2 in fresh YPD and grown at 30°C for 4 hours with constant agitation to establish log phase growth.

Survival analysis post-systemic infection. *C. auris* from log phase or stationary phase cultures were pelleted by centrifugation (5000 rpm for 5min), washed once with sterile PBS, and resuspended in sterile PBS to desired doses for infection. Immunocompetent 8-week old female C57BL/6J mice were infected intravenously with *C. auris* from log phase or stationary phase growth at high dose ($5x10^7$) or low dose ($1x10^6$) via retro-orbital injection in 100 µL volume.

Immediately following infection, mice were monitored for onset of disease symptoms for several hours initially, then daily over the course of 21 days. Mice were sacrificed at a humane endpoint defined as loss of 20 percent of initial bodyweight, or when severe disease symptoms were observed, such as unresponsiveness and labored breathing, or severe neurological symptoms.

Analysis of fungal burden in organs post-mortality. After sacrifice, organs samples were harvested to measure fungal burden. The right lung, right kidney, and spleen were harvested by dissection and homogenized by bead beating with sterile ⅛ inch ball bearings (Grainger 4RJL3) for 10 seconds. Serial dilutions were performed and plated on YPD agar with ampicillin (100 mg/mL) and gentamicin (50 mg/mL). Fungal colonies were grown for 2 days at 30°C and counted, and fungal burdens per organ were calculated.

Histological analysis in organs post-mortality. After sacrifice, organs samples were harvested to perform histological analysis. The left lung and left kidney were harvested by dissection and fixed in 10 percent formalin for 24 hours, then plunged in 70 percent ethanol prior to sectioning and staining (H&E and PAS) by the University of Michigan Orthopaedic Research Laboratories Histology Core. Slides were imaged using a BioTek Lionheart FX automated microscope.

ELISA. After sacrifice, serum was collected by cardiac puncture, followed by isolation of serum using centrifugation (8000g for 5 minutes) of lithium heparin serum collection tubes (Kent Scientific KMIC-LIHEP). Serum samples were submitted to the University of Michigan Cancer Center Immunology Core for quantification of Fibrinogen, TNF, IL-6, and IL-1β by ELISA.

Analysis of cell wall content. Log and stationary phase *C. auris* cells were pelleted by centrifugation (3000 x g for 5 minutes), washed once in PBS, and fixed in 4% paraformaldehyde for 15 minutes. Following fixation, *C. auris* cells were pelleted by centrifugation (3000 x g for 5 minutes), washed twice in PBS, and then stained for cell wall contents, followed by flow cytometry analysis. To quantify mannan content, cells were stained with 5 µg/mL of FITC-Concanavalin A (MilliporeSigma, C7642) for 30 minutes. To quantify exposed β-1,3-glucan, cells were blocked with 3% bovine serum albumin & 5% normal goat serum (Invitrogen, 10000C) for 30 minutes. After blocking, cells were stained with 15 µg/mL of hDectin-1a (InvivoGen, fc-hec1a-2) for 1 hour. Cells were washed twice with PBS before secondary staining with 4 mg/mL of goat raised anti-human IgG antibody conjugated with Alexa Fluor 647 (Invitrogen A-21445) for 30 minutes. To quantify chitin content, cells were stained with 0.1 g/L of Calcofluor White (MilliporeSigma, 18909-100ML-F) for 10 minutes. Following staining, cells were washed with 500µL PBS three times and resuspended in 500µL PBS. Samples were analyzed on a LSRFortessa Flow Cytometer (BD Bioscience, NJ, USA) using BD FACSDiva Software. 10,000 events were recorded for each sample. FlowJo software was used to determine mean fluorescence intensity.

Acknowledgements

We thank Joel Whitfield of the University of Michigan Cancer Center Immunology Core and Emma Snyder-White of the University of Michigan Orthopaedic Research Laboratories Histology Core (NIH P30 AR069620) for guidance and technical support for ELISA and histological analysis, and members of the O'Meara lab for discussion. This work was supported by National Institutes of Health grants U19AI181767 and the Burroughs Wellcome Fund Investigators in Pathogenesis award 1173374 to TRO.

REFERENCES

1. Ortiz-Roa C, Valderrama-Rios MC, Sierra-Umaña SF, Rodríguez JY, Muñetón-López GA, Solórzano-Ramos CA, Escandón P, Alvarez-Moreno CA, Cortés JA. 2023. Mortality caused by Candida auris bloodstream infections in comparison with other Candida species, a multicentre retrospective cohort. J Fungi (Basel) 9.

2. Kim HY PhD, Nguyen TA MSc, Kidd S PhD, Chambers J MD, Alastruey-Izquierdo A PhD, Shin J-H MD, Dao A PhD, Forastiero A MD, Wahyuningsih R MD, Chakrabarti A MD, Beyer P, Gigante V PhD, Beardsley J PhD, Sati H PhD, Morrissey CO PhD, Alffenaar J-W PhD. 2024. Candida auris-a systematic review to inform the world health organization fungal priority pathogens list. Med Mycol 62.

3. Wang Y, Zou Y, Chen X, Li H, Yin Z, Zhang B, Xu Y, Zhang Y, Zhang R, Huang X, Yang W, Xu C, Jiang T, Tang Q, Zhou Z, Ji Y, Liu Y, Hu L, Zhou J, Zhou Y, Zhao J, Liu N, Huang G, Chang H, Fang W, Chen C, Zhou D. 2022. Innate immune responses against the fungal pathogen Candida auris. Nat Commun 13:3553.

4. Xin H, Mohiuddin F, Tran J, Adams A, Eberle K. 2019. Experimental mouse models of disseminated Candida auris infection. mSphere 4.

5. Eix EF, Nett JE. 2025. Candida auris: Epidemiology and antifungal strategy. Annu Rev Med 76:57–67.

6. Santana DJ, Anku JAE, Zhao G, Zarnowski R, Johnson CJ, Hautau H, Visser ND, Ibrahim AS, Andes D, Nett JE, Singh S, O'Meara TR. 2023. A Candida auris-specific adhesin, Scf1, governs surface association, colonization, and virulence. Science 381:1461–1467.

7. Iyer KR, Camara K, Daniel-Ivad M, Trilles R, Pimentel-Elardo SM, Fossen JL, Marchillo K, Liu Z, Singh S, Muñoz JF, Kim SH, Porco JA Jr, Cuomo CA, Williams NS, Ibrahim AS,

Edwards JE Jr, Andes DR, Nodwell JR, Brown LE, Whitesell L, Robbins N, Cowen LE. 2020. An oxindole efflux inhibitor potentiates azoles and impairs virulence in the fungal pathogen Candida auris. Nat Commun 11:6429.

8. Singh S, Uppuluri P, Mamouei Z, Alqarihi A, Elhassan H, French S, Lockhart SR, Chiller T, Edwards JE Jr, Ibrahim AS. 2019. The NDV-3A vaccine protects mice from multidrug resistant Candida auris infection. PLoS Pathog 15:e1007460.

9. Zhao G, Lyu J, Veniaminova NA, Zarnowski R, Mattos E, Johnson CJ, Quintanilla D, Hautau H, Hold LA, Xu B, Anku JAE, Steltzer SS, Dasgupta K, Santana DJ, Ibrahim A, Andes D, Nett JE, Singh S, Abraham AC, Killian ML, Kahlenberg JM, Wong SY, O'Meara TR. 2025. *Candida auris*skin colonization is mediated by Als4112 and interactions with host extracellular matrix proteins. bioRxiv.

10. Herrada J, Roberts K, Gamal A, Long L, Ghannoum MA. 2022. An immunocompromised mouse model of Candida auris systemic infection. Methods Mol Biol 2517:317–328.

11. Torres SR, Pichowicz A, Torres-Velez F, Song R, Singh N, Lasek-Nesselquist E, De Jesus M. 2020. Impact of Candida auris Infection in a Neutropenic Murine Model. Antimicrob Agents Chemother 64.

12. Fakhim H, Vaezi A, Dannaoui E, Chowdhary A, Nasiry D, Faeli L, Meis JF, Badali H. 2018. Comparative virulence of Candida auris with Candida haemulonii, Candida glabrata and Candida albicans in a murine model. Mycoses 61:377–382.

13. Wang X, Bing J, Zheng Q, Zhang F, Liu J, Yue H, Tao L, Du H, Wang Y, Wang H, Huang G. 2018. The first isolate of Candida auris in China: clinical and biological aspects. Emerg Microbes Infect 7:93.

14. Hammer BK, Swanson MS. 1999. Co-ordination of legionella pneumophila virulence with entry into stationary phase by ppGpp. Mol Microbiol 33:721–731.

15. Roop RM 2nd, Gee JM, Robertson GT, Richardson JM, Ng W-L, Winkler ME. 2003. Brucella stationary-phase gene expression and virulence. Annu Rev Microbiol 57:57–76.

16. Wilson JA, Gulig PA. 1998. Regulation of the spvR gene of the Salmonella typhimurium virulence plasmid during exponential-phase growth in intracellular salts medium and at stationary phase in L broth. Microbiology 144 (Pt 7):1823–1833.

17. Ribardo DA, McIver KS. 2003. amrA encodes a putative membrane protein necessary for maximal exponential phase expression of the Mga virulence regulon in Streptococcus pyogenes: Exponential phase expression of Mga. Mol Microbiol 50:673–685.

18. Levi M, van der Poll T. 2017. Coagulation and sepsis. Thromb Res 149:38–44.

19. Litvinov RI, Pieters M, de Lange-Loots Z, Weisel JW. 2021. Fibrinogen and fibrin. Subcell Biochem 96:471–501.

20. Gulla KC, Gupta K, Krarup A, Gal P, Schwaeble WJ, Sim RB, O'Connor CD, Hajela K. 2010. Activation of mannan-binding lectin-associated serine proteases leads to generation of a fibrin clot: MASPs generate a fibrin clot. Immunology 129:482–495.

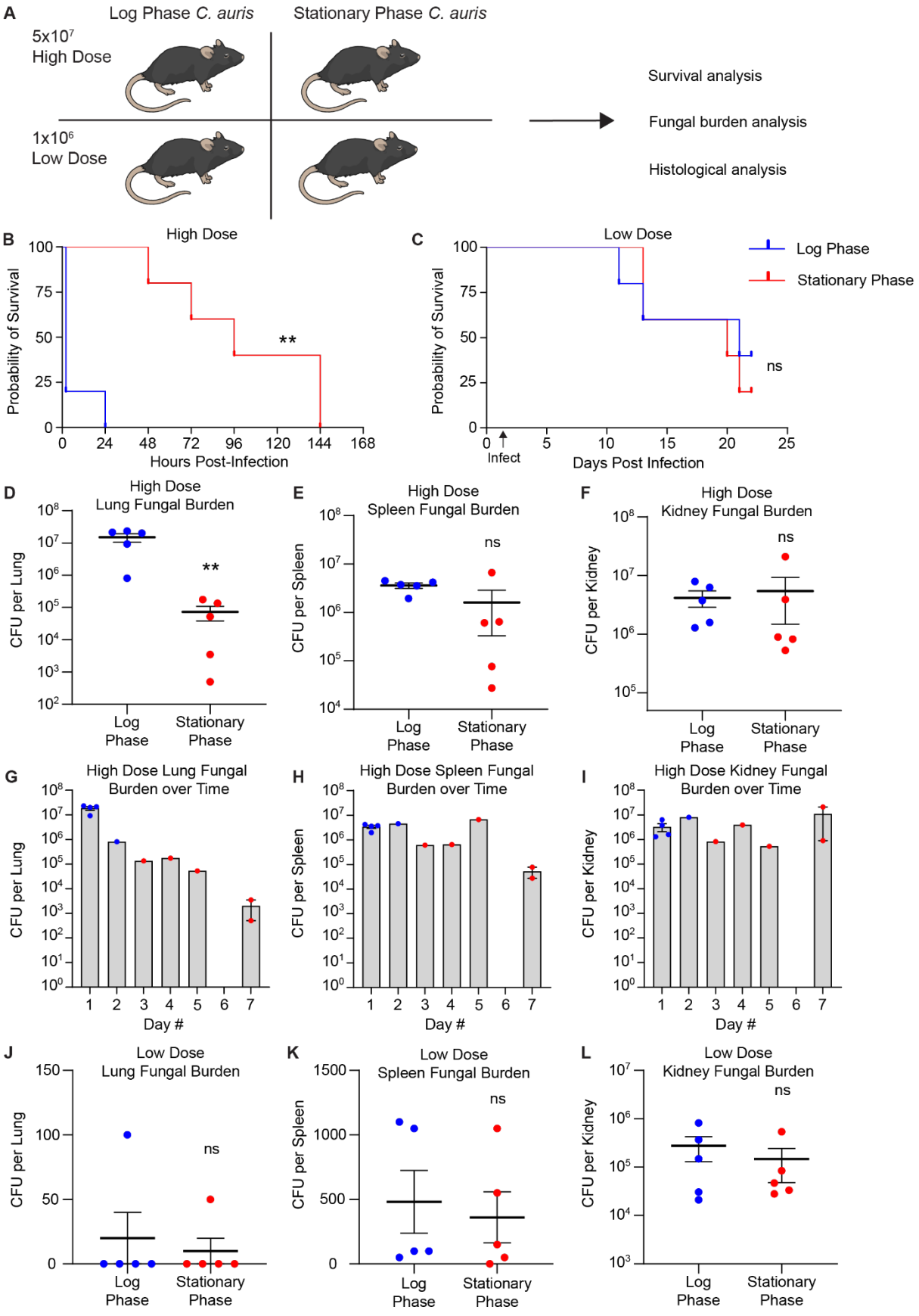

267

Figure 1: *Candida auris* growth phase influences survival kinetics after systemic infection. **(A)** Experimental scheme: Immunocompetent C57BL/6J mice (n=5 per cohort) were infected with a high dose ($5x10^7$) or low dose ($1x10^6$) of B11109 *C. auris* in log phase or stationary phase growth, and survival was monitored. Fungal burden and histological analysis were performed in select organs post-mortality. **(B-C)** Survival probability plots comparing log and stationary phase high dose *C. auris* infection (B) or low dose *C. auris* infection (C). **(D-F)** Post-mortality fungal burden analysis from lung (D), spleen (E), or kidney samples (F) in high dose cohorts. **(G-I)** Post-mortality fungal burden analysis from lung (G), spleen (H), or kidney samples (I) in high dose cohorts plotted as a function of time. Blue dots represent the log phase-infected cohort and red dots represent the stationary phase-infected cohort. **(J-L)** Post-mortality fungal burden analysis from lung (J), spleen (K), or kidney samples (L) in low dose cohorts. * $p<0.05$, ** $p<0.01$, ns not significant by Mantel-Cox test (B-C) or Student's unpaired t test (E-F, J-L).

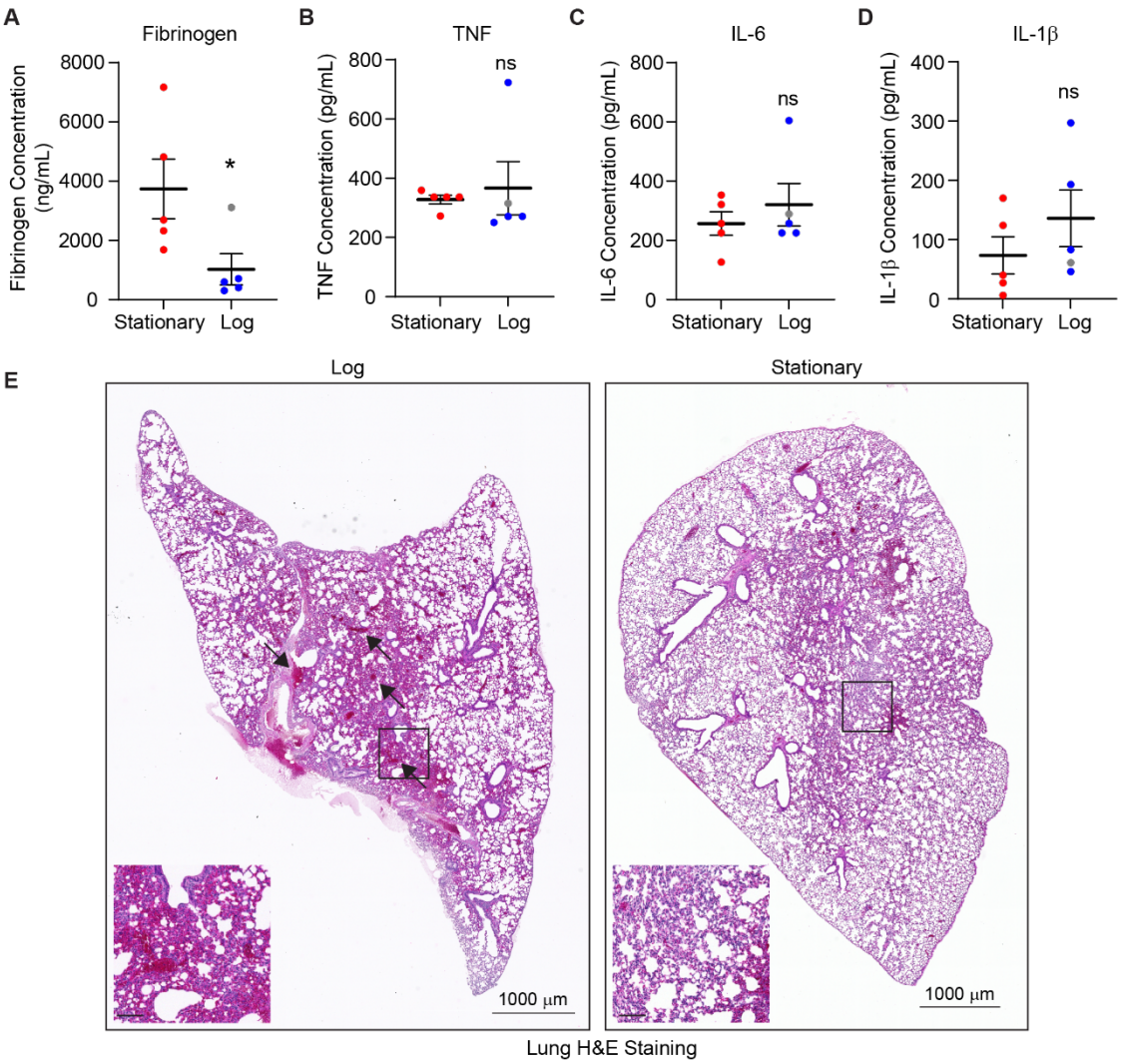

282

Figure 2: Systemic infection with log phase *Candida auris* at high dose triggers rapid blood clotting. (A-D) ELISA data showing levels of Fibrinogen (A), TNF (B), IL-6 (C), and IL-1β (D) from mouse plasma samples harvested post-mortality. Gray data point denotes the mouse within the log phase high dose cohort that survived until day 1 post-infection. **(E)** Representative hematoxylin and eosin (H&E) staining of lung sections from mice in high dose cohorts infected with log phase (left) or stationary phase (right) *C. auris*. Arrows denote blood clots in the lung. Boxes show a magnified inset (scale bar 100 μm). **(F-H)** Representative plots from flow cytometry analysis of *C. auris* cell wall components: β-glucan (measured by human Dectin-1 binding), mannan (measured with concanavalin A-FITC), and chitin (measured with calcofluor white). **(I-K)** Quantification of mean fluorescence intensity of cell wall component staining from flow cytometry analysis, as in F-H: β-glucan (I), mannan (J), and chitin (K). * $p<0.05$, ** $p<0.01$, ns not significant by Student's unpaired t test.